Nonlinear quantum heat transfer in hybrid structures: Sufficient conditions for thermal rectification

Lian-Ao Wu,[1,2] Claire X. Yu,[2] and Dvira Segal[2]
[1]*Department of Theoretical Physics and History of Science, University of the Basque Country UPV/EHU and IKERBASQUE, Basque Foundation of Science, Bilbao, Spain*
[2]*Chemical Physics Group, Department of Chemistry and Center for Quantum Information and Quantum Control, University of Toronto, 80 St. George Street, Toronto, Ontario, Canada M5S 3H6*
(Received 21 May 2009; revised manuscript received 24 July 2009; published 2 October 2009)

We present a unified description of heat flow in two-terminal hybrid quantum systems. Using simple models, we analytically study nonlinear aspects of heat transfer between various reservoirs—metals, solids, and spin baths—mediated by the excitation and the relaxation of a central (subsystem) mode. We demonstrate rich nonlinear current-temperature characteristics, originating from either the molecular anharmonicity or the reservoir (complex) energy spectra. In particular, we establish sufficient conditions for thermal rectification in two-terminal junctions. We identify two classes of rectifiers. In type-*A* rectifiers the energy-dependent density of states of the reservoirs are dissimilar. In type-*B* rectifiers the baths are identical, but include particles whose statistics differ from that of the subsystem, to which they asymmetrically couple. Nonlinear heat flow and specifically thermal rectification are thus ubiquitous effects that could be observed in a variety of systems—phononic, electronic, and photonic.

DOI: 10.1103/PhysRevE.80.041103 PACS number(s): 05.60.Gg, 63.22.−m, 44.10.+i, 66.70.−f

I. INTRODUCTION

Understanding heat transfer in two-terminal hybrid structures is of fundamental and practical importance for controlling transport at the nanoscale and for realizing functional devices [1,2]. Among the systems that fall into this category are metal-molecule-metal junctions, the basic component of molecular electronic devices. Here, the excessive energy generated at the molecular core should be effectively removed for realizing a stable device, as demonstrated theoretically [3] and experimentally [4,5]. Another composite structure of fundamental interest is a dielectric-molecule-dielectric system, where vibrational energy flowing between the components activates reactivity and controls dynamics [6–8]. Phononic junctions are also captivating for understanding the validity of Fourier's law of thermal conduction at the nanoscale [9,10]. Single-mode *radiative* heat conduction between Ohmic metals was recently detected, manifesting that photon-mediated thermal conductance is quantized [11]. Other hybrid systems with interesting thermal properties are electronic-spin–nuclear-spin interfaces [12], metal-molecule-dielectric contacts [13], and metal-superconductor junctions [14].

From the theoretical point of view, the basic challenge here is to understand the role of nonlinear interactions in determining transport mechanisms and, specifically, in inducing normal (Fourier) heat conduction, either within classical laws [9,15,16] or based on quantum-mechanical principles [17–22]. The treatments employed vary. Ballistic heat transfer in phononic systems was explored using the Landauer-scattering formalism [23] and within the generalized Langevin equation [16,24,25]. For interacting systems there are only few analytical results, and the techniques employed include the kinetic-Boltzmann theory [26], mode-coupling theory [27,28], the nonequilibrium Green's-function method [21,29,30], classical [15] and mixed classical-quantum [31] molecular-dynamics simulations, and exact quantum simulations on simplified models [32].

The master-equation formalism [33] is another useful tool for studying quantum heat transfer across nanojunctions [34–36]. We have recently adopted this method in the weak system-bath coupling limit and explored various aspects of heat flow in simplified toy models [20,37–39]. Basically, we ask ourselves the following question: what is the connection between the microscopic Hamiltonian and the heat current across the system? More specifically, how can we control the onset of nonlinear current-temperature behavior [37,38] and what conditions should the Hamiltonian satisfy for the system to manifest normal conduction [20]? While our treatment has been typically limited to a minimal subsystem, the formalism has two main advantages: (i) both harmonic and anharmonic systems can be treated within the same footings and (ii) analytical results obtained can pinpoint on the underlying dynamics, typically obscured in numerical simulations.

In this work we extend our recent letters [39,40], broaden our scope beyond the (nonlinear) thermal rectifying effect, and develop a *unified* description of temperature-driven quantum heat transfer at the nanoscale. We focus on two-terminal devices, including a central quantized unit (subsystem) and two bulk objects (referred to as terminals, contacts, reservoirs, or baths), whose temperatures are externally controlled. Our description can be applied on several systems, including electron-hole pair excitations, phonons, photons, or spins. However, our formalism does not describe the heat flow due to the transport of hot charge carriers [3].

We analytically explore current-temperature characteristics in various systems and seek to connect the nonlinear behavior to the microscopic parameters: the system energetics, the reservoirs characteristics, and the junction asymmetry. We investigate the temperature dependence of the thermal conductance and observe a rich behavior, depending of the details of the model. We also demonstrate that the sub-

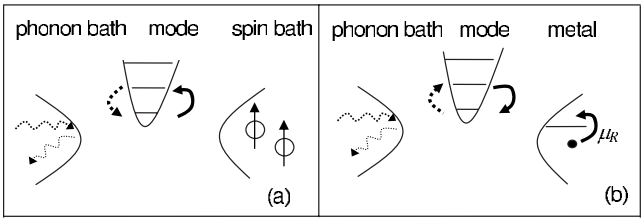

FIG. 1. Examples of two hybrid systems treated in this work. (a) Single-mode heat transfer between a solid and a spin bath. The central unit can represent either a vibrational or a radiation mode. (b) Phonon to exciton energy exchange.

system temperature in nonequilibrium situations is a sensitive witness for the onset of nonlinear interactions in the transport process.

In particular, we discuss two simple nonlinear effects: thermal rectification, an asymmetry of the heat current for forward and reversed temperature gradients, and a negative differential thermal conductance (NDTC), where the current goes down with increasing bias. While in the weak-system-bath coupling limit employed NDTC is typically absent, we observe the rectification phenomenon in various junctions.

Thermal rectification has recently attracted considerable theoretical [37,41–50] and experimental [51,52] attention. While most theoretical studies have analyzed this phenomenon in *phononic systems* using classical molecular-dynamics simulations, our prototype model can describe thermal rectification of several subsystems (vibrational or radiation modes) and reservoirs (spin, metal, and dielectrics) at the same footing (see Fig. 1). Moreover, using our simple model we establish *sufficient* conditions for rectification [40]. We identify two classes of rectifiers: (i) "type A," where the reservoirs are dissimilar, i.e., of different (energy-dependent) densities of states (DOSs) (this condition is more general than the one discussed in Ref. [40]) and (ii) "type B," where the baths are identical, but their statistics differ from that of the subsystem, combined with unequal coupling strengths at the two ends, as explained below.

The content of the paper is as follows. In Sec. II we present our model. In Sec. III we derive equations of motion for the subsystem population using the quantum master-equation approach. We consider several models for the subsystem and for the contacts and derive analytical expressions for the heat current. In Sec. IV we trace these junctions' (nonlinear) current-temperature characteristics to the Hamiltonian parameters. In particular, Sec. V is focused on a specific nonlinear effect: thermal rectification. We analytically identify two types of rectifiers and demonstrate with numerical simulations the tunability of the effect. Conclusions follow in Sec. VI.

II. MODEL

We consider generic hybrid structures where a central unit H_S interacts with two reservoirs H_ν^0 ($\nu=L,R$) of temperatures $T_\nu=\beta_\nu^{-1}$ ($k_B\equiv 1$) via the coupling terms V_ν,

$$H = H_L^0 + H_R^0 + H_S + V_L + V_R. \tag{1}$$

The heat current from the ν bath into the subsystem is given by [53], $J_\nu=\frac{i}{2}\mathrm{Tr}([H_\nu^0-H_S,V_\nu]\rho)$ ($\hbar\equiv 1$), where ρ is the total density matrix, and we trace over both the subsystem and the reservoir degrees of freedom. In steady state the expectation value of the interaction is zero, $\mathrm{Tr}[(\partial V_\nu/\partial t)\rho]=0$, and we obtain

$$J_L = i\,\mathrm{Tr}([V_L,H_S]\rho), \quad J_R = i\,\mathrm{Tr}([V_R,H_S]\rho). \tag{2}$$

Since in steady state the currents are equal, $J_L=-J_R$, we introduce a symmetric definition for the heat current operator $\hat{J}$,

$$J = \mathrm{Tr}[\hat{J}\rho], \quad \hat{J} = \frac{i}{2}[V_L,H_S] + \frac{i}{2}[H_S,V_R], \tag{3}$$

where the expectation value is defined positive when the current is flowing from L to R. The subsystem Hamiltonian assumes a diagonal form, and we also consider separable couplings

$$H_S = \sum_n E_n|n\rangle\langle n|,$$

$$V_\nu = \lambda_\nu S B_\nu, \quad S = \sum_{n,m} S_{m,n}|m\rangle\langle n|. \tag{4}$$

Here, S is a subsystem operator and B_ν is an operator in terms of the ν bath degrees of freedom. For simplicity we set $S_{m,n}=S_{n,m}$. In what follows we consider situations where B_L and B_R have the same dependence on the (respective) bath degrees of freedom, with different prefactors $\lambda_L\neq\lambda_R$. We refer to this scenario as "parametric asymmetry," rather than "functional asymmetry," resulting from dissimilar B's. Note that, if the commutator $[H_S,S]=0$, the heat current trivially vanishes.

III. DYNAMICS

Employing the Liouville equation in the interaction picture, the elements of the total density matrix satisfy

$$\frac{d\rho_{m,n}}{dt} = -i[V(t),\rho(0)]_{m,n} - \int_0^t d\tau[V(t),[V(\tau),\rho(\tau)]]_{m,n}, \tag{5}$$

where $V=V_L+V_R$ and $V(t)$ are interaction picture operators. Following standard weak-coupling schemes [33], we proceed by making four assumptions. (i) We first make the presumption that $\mathrm{Tr}[V(t),\rho(0)]=0$, i.e., the mean value of the interaction Hamiltonian, averaged over the initial density matrix, is zero. (ii) We factorize the density matrix of the whole system, at all times, by the product $\rho(t)=\sigma(t)\rho_L(T_L)\rho_R(T_R)$. Here, ρ_ν is independent of time, $\rho_\nu(T_\nu)=e^{-H_\nu^0/T_\nu}/\mathrm{Tr}_\nu[e^{-H_\nu^0/T_\nu}]$, and $\sigma(t)$ is the subsystem density matrix obtained by tracing out the reservoirs degrees of freedom from the total density matrix, $\sigma(t)=\mathrm{Tr}_B[\rho(t)]$. Tr_B denotes trace over both the L and the R bath degrees of freedom. (iii) We take the Markovian limit, assuming that the reservoirs' characteristic time scales are shorter than the subsystem relaxation time. (iv) We neglect contributions from quantum coherences, i.e., in the long-time limit we assume that the nondiagonal elements of

the system density matrix vanish. This can be justified in the weak-coupling limit adopting the initial condition $\sigma_{n\neq m}(0)\sim 0$. Following these assumptions, the Pauli master equation for the populations $P_n(t)=\mathrm{Tr}_B[\rho_{n,n}(t)]$ is obtained as [33]

$$\dot{P}_n(t)=\sum_{\nu,m}|S_{m,n}|^2P_m(t)k^{\nu}_{m\to n}(T_\nu)-P_n(t)\sum_{\nu,m}|S_{m,n}|^2k^{\nu}_{n\to m}(T_\nu). \tag{6}$$

The Fermi golden rule transition rates are given by

$$k^{\nu}_{n\to m}(T_\nu)=\lambda_\nu^2\int_{-\infty}^{\infty}d\tau\, e^{iE_{n,m}\tau}\langle B_\nu(\tau)B_\nu(0)\rangle_{T_\nu}. \tag{7}$$

Here, $E_{m,n}=E_m-E_n$ and $\langle B_\nu(\tau)B_\nu(0)\rangle_{T_\nu}=\mathrm{Tr}_\nu[\rho_\nu(T_\nu)B_\nu(\tau)B_\nu(0)]$ is the correlation function of the ν environment. In steady state $\dot{P}_n=0$, and we normalize the population to unity $\Sigma_n P_n=1$. It is straightforward to show that under Eq. (4) the steady-state current (3) becomes

$$J=\frac{1}{2}\sum_{n,m}E_{m,n}|S_{m,n}|^2P_n\times[k^L_{n\to m}(T_L)-k^R_{n\to m}(T_R)], \tag{8}$$

with the population obtained by solving Eq. (6) in the long-time limit. For details see the Appendix. Our description to this point is general, as we have not yet specified either the subsystem or the terminals.

A. Specific models for the subsystem Hamiltonian

We consider two representative models for the subsystem Hamiltonian and its interaction with the baths. In the first model the subsystem is a harmonic oscillator (HO) of frequency ω, $H_S=\Sigma_n n\omega|n\rangle\langle n|$. This can describe either a local radiation mode [11,39] or an active vibrational mode of the trapped molecule [38]. For the interaction operator we assume $S=\Sigma_n\sqrt{n}|n\rangle\langle n-1|+\mathrm{c.c.}$, motivated by the bilinear form $V_\nu\propto xB_\nu$, where x is a subsystem coordinate [38]. This implies that only transitions between nearest states are allowed,

$$k^{\nu}(T_\nu)\equiv k^{\nu}_{n\to n-1}(T_\nu)=\lambda_\nu^2\int_{-\infty}^{\infty}d\tau\, e^{i\omega\tau}\langle B_\nu(\tau)B_\nu(0)\rangle_{T_\nu},$$

$$k^{\nu}_{n-1\to n}(T_\nu)=e^{-\beta_\nu\omega}k^{\nu}_{n\to n-1}(T_\nu). \tag{9}$$

We also introduce the short notation

$$k^{\nu}(T_\nu)=\lambda_\nu^2 f_\nu(T_\nu), \tag{10}$$

where f_ν, defined through Eq. (9), encompasses the effect of the bath operators. Solving Eq. (6) in steady state using the above expressions for the rates, the heat current (8) can be analytically calculated as [37]

$$J^{(HO)}=-\frac{\omega[n^L_B(\omega)-n^R_B(\omega)]}{n^L_B(-\omega)/k^L(T_L)+n^R_B(-\omega)/k^R(T_R)}, \tag{11}$$

where $n^\nu_B(\omega)=[e^{\beta_\nu\omega}-1]^{-1}$ is the Bose-Einstein distribution function at $T_\nu=1/\beta_\nu$.

Our second subsystem is a two-level (spin) system (TLS). Here, $H_S=\frac{\omega}{2}\sigma_z$, and we employ a nondiagonal interaction form $S=\sigma_x$. These terms can represent an electronic spin rotated by the environment [12]. It can also describe an anharmonic (truncated) molecular vibration that is dominating heat flow through the junction [37,38]. Recalculating the long-time population (6), the heat flux reduces to

$$J^{(TLS)}=\frac{\omega[n^L_S(\omega)-n^R_S(\omega)]}{n^L_S(-\omega)/k^L(T_L)+n^R_S(-\omega)/k^R(T_R)} \tag{12}$$

with the rates (9) and the spin occupation factor $n^\nu_S(\omega)=[e^{\beta_\nu\omega}+1]^{-1}$.

Expressions (11) and (12) demonstrate that in the weak-coupling limit the effect of the environment enters only through the relaxation rates k^ν, evaluated at the subsystem energy spacing ω. In Sec. IV we further introduce a three-level system (3LS), an intermediate structure between a two-level (strongly anharmonic) system, and a harmonic object. More generally, given the subsystem anharmonic potential and an interaction operator S, one should proceed by (i) calculating (analytically or numerically) the vibrational spectra $|n\rangle$, (ii) evaluating the matrix elements of S, (iii) acquiring the steady-state levels populations by solving Eq. (6), and (iv) arriving at the heat current using Eq. (8).

B. Calculation of the rate constant

We give next the explicit form for the relaxation rate for various physical thermal baths. The rate constants (9) induced by, e.g., the L contact is given by the Fourier transform of the bath correlation function $\langle B_L(\tau)B_L(0)\rangle_{T_L}$, with $B_L=\Sigma B^L_{l,l'}|l\rangle\langle l'|$ and $H^0_L=\Sigma E_l|l\rangle\langle l|$. Here, $|l\rangle$ are the many-body states of the L reservoir with energies E_l. Rate (9) can be integrated to yield

$$k^\nu(T_\nu)=2\pi\lambda_\nu^2\sum_{j,j'}|B^\nu_{j,j'}|^2\delta(E_j-E_{j'}+\omega)\frac{e^{-\beta_\nu E_j}}{Z_\nu(\beta_\nu)}, \tag{13}$$

with $Z_\nu(\beta_\nu)=\Sigma_j e^{-\beta_\nu E_j}$ as the partition function of the ν bath; $j,j'\in\nu$.

1. Distinguishable noninteracting particles

This environment includes a set of independent ($p=1,2,\ldots,P$) particles. The Hamiltonian is given by summing all separate contributions

$$H^0_\nu=\sum_p h^0_{\nu,p},\quad B_\nu=\sum_p b_{\nu,p}. \tag{14}$$

Within these terms, the relaxation rate (13) reduces to

$$k^\nu(T_\nu)=2\pi\lambda_\nu^2\sum_p\sum_{i,j}|\langle i|_p b_{\nu,p}|j\rangle_p|^2\delta(\epsilon_p(i)-\epsilon_p(j)+\omega)\frac{e^{-\beta_\nu\epsilon_p(i)}}{Z_p(\beta_\nu)}, \tag{15}$$

with the p-particle eigenstates $|i\rangle_p$ and eigenvalues $\epsilon_p(i)$. $Z_p(\beta_\nu)=\Sigma_i e^{-\beta_\nu\epsilon_p(i)}$ is the p-particle partition function. Specifically, for a bath of noninteracting spins (states $|0\rangle_p$ and $|1\rangle_p$ we get

$$k^\nu(T_\nu)=\Gamma^\nu_S(\omega)n^\nu_S(-\omega), \tag{16}$$

with the spin occupation factor $n_S^\nu(\omega)=[e^{\beta_\nu\omega}+1]^{-1}$ and the temperature-independent coefficient

$$\Gamma_S^\nu(\omega)=2\pi\lambda_\nu^2\sum_p |\langle 0|_p b_{\nu,p}|1\rangle_p|^2\delta(\omega+\epsilon_p(0)-\epsilon_p(1)). \quad (17)$$

2. Harmonic bath: Solid or radiation field

This bath includes a set of independent harmonic-oscillators with creation operators $a_{\nu,j}^\dagger$. System-bath interactions are further assumed to include the oscillator displacements,

$$H_\nu^0=\sum_j \omega_j a_{\nu,j}^\dagger a_{\nu,j}, \quad B_\nu=\sum_j (a_{\nu,j}+a_{\nu,j}^\dagger). \quad (18)$$

This leads to the relaxation rate

$$k^\nu(T_\nu)=-\Gamma_B^\nu(\omega)n_B^\nu(-\omega), \quad (19)$$

with the Bose-Einstein function $n_B^\nu(\omega)=[e^{\beta_\nu\omega}-1]^{-1}$ and an effective system-bath coupling factor

$$\Gamma_B^\nu(\omega)=2\pi\lambda_\nu^2\sum_j \delta(\omega_j-\omega). \quad (20)$$

3. Fermionic bath: Metal

Consider a metallic terminal including a set of noninteracting spinless electron creation operators $c_{\nu,i}^\dagger$, where only scattering between electronic states within the same lead are allowed,

$$H_\nu^0=\sum_i \epsilon_i c_{\nu,i}^\dagger c_{\nu,i}, \quad B_\nu=\sum_{i,j} c_{\nu,i}^\dagger c_{\nu,j}. \quad (21)$$

The transition rate between subsystem states (13) can be written as [13]

$$k^\nu(T_\nu)=-2\pi\lambda_\nu^2 n_B^\nu(-\omega)\sum_{i,j}\delta(\epsilon_i-\epsilon_j+\omega)[n_F^\nu(\epsilon_i)-n_F^\nu(\epsilon_i+\omega)], \quad (22)$$

with the Fermi-Dirac distribution function $n_F^\nu(\epsilon)=[e^{\beta_\nu(\epsilon-\mu_\nu)}+1]^{-1}$, where μ_ν is the chemical potential. One could also write

$$k^\nu(T_\nu)=-\Lambda^\nu(T_\nu,\omega)n_B^\nu(-\omega), \quad (23)$$

where

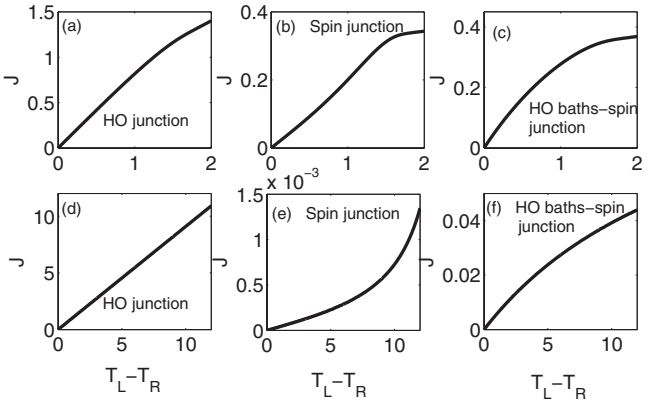

FIG. 2. Nonlinear heat flow in various hybrid junctions. (a)–(c) $\omega=1$, $T_a=2$. (d)–(f) $\omega=0.1$, $T_a=15$. (a) and (d) are harmonic junctions with the current (29); (b) and (e) are spin junctions obeying Eq. (30); (c) and (f) are harmonic bath-spin junctions obeying Eq. (31). $\Gamma^L=10$, $\Gamma^R=1$ in all figures. The x axis is ΔT.

$$\Lambda^\nu(T_\nu,\omega)=2\pi\int d\epsilon[n_F^\nu(\epsilon)-n_F^\nu(\epsilon+\omega)]F_\nu(\epsilon). \quad (24)$$

The function $F_\nu(\epsilon)=\lambda_\nu^2\Sigma\delta(\epsilon-\epsilon_j+\omega)\delta(\epsilon_i-\epsilon)$ depends on the system-bath coupling elements and the specific band structure. Assuming that the density of states slowly varies in the (subsystem) energy window ω, the interaction function can be expanded around the chemical potential [13] $F_\nu(\epsilon)\approx F_\nu(\mu_\nu)+\gamma_\nu[(|\epsilon|-\mu_\nu)/\mu_\nu]$, with γ_ν as a dimensionless number of order unity. Using this form, the integration in Eq. (24) can be performed when the Fermi energy is much bigger than the conduction band edge $\mu_\nu \gg E_c$. One can then write

$$\Lambda^\nu(T_\nu,\omega)\approx\Gamma_F^\nu(\omega)\left(1+\delta_\nu\frac{T_\nu}{\mu_\nu}\right), \quad (25)$$

where δ is a constant of order 1, measuring the deviation from a flat band structure near the chemical potential μ_ν [39]. The coupling constant is given by

$$\Gamma_F^\nu(\omega)=2\pi\omega F_\nu(\mu_\nu). \quad (26)$$

When $\delta_\nu=0$ we find that $\Lambda^\nu(T_\nu,\omega)=\Gamma_F^\nu(\omega)$, a temperature-independent constant, and the harmonic limit (19) is retrieved [39].

To conclude this discussion, assuming different types of reservoirs and system-bath couplings, we derived here three expressions for the relaxation rate (13) [or equivalently Eq. (9)]: Eq. (16) assuming a spin bath, Eq. (19) for a phononic environment with a linear coupling to the subsystem, and Eq. (23) for a metallic bulk with electron-hole pair excitations

$$k^\nu(T_\nu)=\begin{cases} n_S^\nu(-\omega)\Gamma_S^\nu(\omega), & \text{noninteracting spins} \\ -n_B^\nu(-\omega)\Gamma_B^\nu(\omega), & \text{phonons, linear coupling} \\ -n_B^\nu(-\omega)\left(1+\delta_\nu\dfrac{T_\nu}{\mu_\nu}\right)\Gamma_F^\nu(\omega), & \text{metal.} \end{cases} \quad (27)$$

In each case the coefficient Γ^{ν} reflects temperature-independent system-bath interaction strength, whereas the temperature-dependent function reflects the reservoir properties only.

IV. NONLINEAR CURRENT-TEMPERATURE CHARACTERISTICS

Based on the two models for the subsystem (HO and TLS) and the different types of baths, we can construct several two-terminal heat-conducting junctions. We consider next few examples and manifest nonlinear current-temperature behavior. We will also introduce a 3LS, an intermediate structure between a two-level (strongly anharmonic) system, and a harmonic object. Formally, if we write the heat current as

$$J(T_a,\Delta T)=\sum_n \alpha_n(T_a)\Delta T^n \tag{28}$$

with $\Delta T=T_L-T_R$, $T_a=T_L+T_R$, we ask ourselves what are the microscopic parameters that are incorporated in the nonlinear coefficients α_n $(n>1)$ and how can we control the magnitude of these terms. We also define the thermal conductance as $\mathcal{K}=\lim_{\Delta T\to 0} J/\Delta T$ and examine its temperature dependence.

A. Harmonic junction

Our first example is a fully harmonic system, incorporating two harmonic reservoirs connected by a harmonic link, modeling vibrational or photonic heat transfer between two solid or Ohmic metals [11,24,54], assuming that a specific harmonic mode of frequency ω dominates the dynamics. The current is given by Eq. (11) with rates (19), resulting in the thermal Landauer expression [23]

$$J=\mathcal{T}_B\omega[n_B^L(\omega)-n_B^R(\omega)] \tag{29a}$$

$$\overset{\beta_\nu\omega\ll 1}{\to} \mathcal{T}_B\left[\Delta T-\frac{\omega^2}{3T_a^4}\Delta T^3+O(\Delta T^5)\right]. \tag{29b}$$

Here, $\mathcal{T}_B=\Gamma_B^L\Gamma_B^R/(\Gamma_B^L+\Gamma_B^R)$ is a (temperature-independent) transmission coefficient, with the coupling elements Γ_B^{ν} calculated at the molecular frequency ω. This equation describes ballistic thermal transport, where energy loss takes place only at the contacts. Note that in the classical limit $J\propto\Delta T$, $\mathcal{K}=\mathcal{T}_B$, and the current does not directly depend on the molecular (subsystem) vibrational frequency only through the coefficient Γ. For a harmonic junction, nonlinear effects are thus purely quantum, originating from the quantum statistics.

B. Spin junction

Our second example is a spin-TLS-spin system representing, e.g., a central electron interacting with two nuclear-spin environments under an applied magnetic field [12]. The current is given by Eq. (12) with rates (16), bringing in a spin-Landauer formula

$$J=\mathcal{T}_S\omega[n_S^L(\omega)-n_S^R(\omega)] \tag{30a}$$

$$\overset{\omega\beta_\nu\ll 1}{\to} \mathcal{T}_S\frac{\omega^2}{T_a}\sum_{n=1,3,5,\ldots}\left(\frac{\Delta T}{T_a}\right)^n, \tag{30b}$$

with the transmission coefficient $\mathcal{T}_S=\Gamma_S^L\Gamma_S^R/(\Gamma_S^L+\Gamma_S^R)$, Γ_S^{ν} is evaluated at ω, the central spin energy spacing. Unlike Eq. (29b), the linear-response term here does depend on the subsystem frequency, $\mathcal{K}=\mathcal{T}_S\omega^2/T_a^2$, and nonlinear terms persist even in the high-temperature limit. Note that both Eqs. (29a) and (30a) are in the form of Landauer formula, since only elastic scattering processes are effective (system and reservoirs are identical). Our next two examples bring in deviations from the Landauer picture.

C. Harmonic bath-spin subsystem junction

Consider again vibrational heat flow. However, unlike the fully harmonic model resulting in Eq. (29), the central unit is assumed here to incorporate anharmonic terms [37,39,50]. This can be implemented by modeling the subsystem by a truncated harmonic oscillator, for example, a spin. The current across the device is evaluated using Eq. (12) with rates (19),

$$J=\omega\frac{\Gamma_B^L\Gamma_B^R[n_B^L(\omega)-n_B^R(\omega)]}{\Gamma_B^L[1+2n_B^L(\omega)]+\Gamma_B^R[1+2n_B^R(\omega)]} \tag{31a}$$

$$\overset{\omega\beta_\nu\ll 1}{\to} \mathcal{T}_B\omega\sum_{n=1}^{\infty}\left(\frac{\Delta T}{T_a}\right)^n(-\chi_B)^{n-1}, \tag{31b}$$

where $\chi_B=(\Gamma_B^L-\Gamma_B^R)/(\Gamma_B^L+\Gamma_B^R)$ measures the spatial asymmetry. Note that we could still organize Eq. (31a) in the form of the Landauer formula with a *temperature-dependent* transmission coefficient [21]. The high-temperature linear-response limit yields $\mathcal{K}=\mathcal{T}_B\omega/T_a$. Nonlinear terms survive in Eq. (31b) *only due to the asymmetric coupling*, since for $\chi_B=0$, $J\propto\Delta T$. Thus, quite interestingly, this anharmonic junction conducts linearly (in the classical limit), as long as it is fully symmetric.

Can we identify a regime where the current *decays* with increasing temperature bias? This highly nonlinear effect is referred to as "negative differential thermal conductance," and we prove next that it is absent in the present model. In the high-temperature regime, we calculate the derivative of Eq. (31b) as

$$\frac{\partial J}{\partial\Delta T}\propto\sum_{n=1}^{\infty}n\left(\frac{\Delta T}{T_a}\right)^{n-1}(-\chi_B)^{n-1}. \tag{32}$$

Assuming that the junction is highly asymmetric, $\Gamma_B^L\gg\Gamma_B^R$, we take $\chi_B\sim 1$ and obtain

$$\frac{\partial J}{\partial\Delta T}\propto 1-2x+3x^2-4x^3+\cdots=\frac{1}{(1+x)^2}, \tag{33}$$

with $x=\Delta T/T_a$. Since this derivative is always positive, the current systematically grows with temperature bias, and the NDTC effect is absent. Note that a pure harmonic model

(30b), as well as a spin model (29a), also precludes NDTC.

In Fig. 2 we exemplify the properties of junctions (29a), (29b), (30a), (30b), (31a), and (31b) with asymmetric couplings $\Gamma^L \neq \Gamma^R$, taking ω, the subsystem characteristic energy, to be either on the order of the reservoirs temperature, $\omega \sim T_a$, or significantly lower. In the first case subplots (a)–(c) reveal that the current saturates at large ΔT, reflecting the quantum statistics. In contrast, in the high-temperature limit, while a pure harmonic system (d) shows a linear current-ΔT characteristic, the other two systems (e) and (f), incorporating some nonlinearities, reveal a nonlinear behavior.

D. Three-level junctions

In order to further elucidate the role of uniform energy spectra in nonlinear transport, we construct next a 3LS, an intermediate structure between a two-level (strongly anharmonic) subsystem, and a harmonic object. We assume that both the subsystem and the reservoirs include (equivalent) 3LS particles, $H_S=\Sigma_{n=1,2,3}E_n|n\rangle\langle n|$, $S=|1\rangle\langle 2|+|2\rangle\langle 3|+\text{H.c.}$ The current (8) reduces to

$$J = \frac{\omega_1}{D_1} k^L_{2\to 1} k^R_{2\to 1} (e^{-\beta_L \omega_1} - e^{-\beta_R \omega_1}) + \frac{\omega_2}{D_2} k^L_{3\to 2} k^R_{3\to 2} (e^{-\beta_L \omega_2} - e^{-\beta_R \omega_2}), \tag{34}$$

with $\omega_1=E_2-E_1$, $\omega_2=E_3-E_2$, and

$$D_1 = k_{1\to 2} k_{2\to 3}/k_{3\to 2} + k_{1\to 2} + k_{2\to 1},$$

$$D_2 = k_{3\to 2} k_{2\to 1}/k_{1\to 2} + k_{3\to 2} + k_{2\to 3}. \tag{35}$$

Here, $k_{i\to j}=k^L_{i\to j}+k^R_{i\to j}$, with the rates defined in Eq. (7). Taking $\omega=\omega_1=\omega_2$, and assuming that the reservoirs include collections of 3LS noninteracting particles of equal spacing ω, we obtain the following expression, using Eq. (15) ($\omega \ll T_a$):

$$J = \frac{16}{9} \frac{\omega^2}{T_a} \mathcal{T}_S \sum_{n=1,3,5,\ldots} \left(\frac{\Delta T}{T_a} \right)^n \tag{36}$$

with $\mathcal{T}_S=\Gamma^L_S\Gamma^R_S/(\Gamma^L_S+\Gamma^R_S)$ and $\Gamma^\nu_S=2\pi\lambda^2_\nu \Sigma_p |\langle i|_p b_{\nu,p}|j\rangle_p|^2 \delta(\omega+\epsilon_p(i)-\epsilon_p(j))$; $i<j$. This expression is essentially similar to Eq. (30). It is notable that only *odd* terms survive, irrespective of the spatial asymmetry ($\Gamma^L \neq \Gamma^R$). It can be shown that even terms participate only when the energy spectra along the device becomes inhomogeneous.

E. Energy flow between metals

Energy transfer between metals, mediated by the excitation of a single radiation mode, has recently attracted considerable experimental and theoretical interests [11,39,50,54]. Analogous junctions are the core of molecular electronics, where the bridging modes are the vibrations of the trapped molecules. For example, heat dissipation in a metal-C_{60}-scanning tunneling microscope (STM) junction was demonstrated to be controlled by vibrational decay into the tip, generating electron-hole pair excitations [4,13]. Heat conduction through a DNA-gold composite, suspended between two electrodes, was found to be dominated by phonon transport [55].

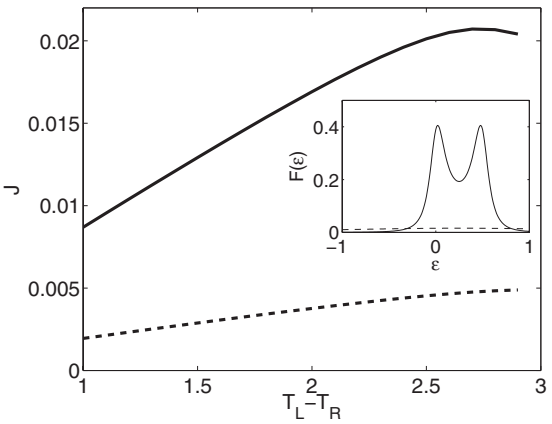

FIG. 3. Negative differential thermal conductance in a metal–single-mode–metal junction with $\gamma=0.2$ (solid line). $\Gamma^L_F=\Gamma^R_F=1$, $T_a=3$, $\omega=0.5$. The dashed curve was generated using $\gamma=5$, manifesting behavior similar to the fully harmonic case (29). Inset: the function $F(\epsilon)$ [see Eq. (24)] vs energy for $\gamma=0.2$ (solid line) and $\gamma=5$ (dashed line).

When both metals are Ohmic, the current in the weak-coupling limit is given by Eq. (29) [39]. As we show next, for structured reservoirs nonlinear effects emerge in the classical limit. We calculate the heat current using Eq. (11) with rates (23)–(25), assuming $\mu=\mu_\nu$ and $\delta=\delta_\nu$, i.e., the reservoirs are equivalent and are maintained at the same chemical potential. This leads to

$$J = \omega \frac{\Gamma^R_F \Gamma^L_F \left(1+\delta\frac{T_L}{\mu}\right)\left(1+\delta\frac{T_R}{\mu}\right)[n^L_B(\omega)-n^R_B(\omega)]}{\Gamma^L_F\left(1+\delta\frac{T_L}{\mu}\right)+\Gamma^R_F\left(1+\delta\frac{T_R}{\mu}\right)} \tag{37a}$$

$$\overset{\omega\beta_\nu \ll 1}{\to} \mathcal{T}_F \left[\left(1+\delta\frac{T_a}{2\mu}\right)\Delta T - \chi_F \frac{\delta}{2\mu}\Delta T^2 - \frac{\delta^2}{\mu^2}\frac{\Gamma^L_F\Gamma^R_F}{(\Gamma^L_F+\Gamma^R_F)^2}\Delta T^3 + O(\Delta T^4) \right]. \tag{37b}$$

In deriving Eq. (37b) we assumed that $\delta T_a/2\mu < 1$. Here, $\chi_F=(\Gamma^L_F-\Gamma^R_F)/(\Gamma^L_F+\Gamma^R_F)$ measures the asymmetry in the system-bath coupling and $\mathcal{T}_F=\Gamma^L_F\Gamma^R_F/(\Gamma^L_F+\Gamma^R_F)$. The following observations can be made. (i) The nonlinear contributions are all related to a finite δ, measuring the deviation from a constant density of states [39]. If $\delta=0$, the harmonic limit is recovered. (ii) The existence of even terms, e.g., a ΔT^2 term, requires some asymmetry, $\chi_F \neq 0$, as we discuss below [see Eq. (51)]. (iii) The conductance of the junction scales like $\mathcal{K}=\mathcal{T}_F(1+\delta T_a/2\mu)$, in sharp contrast to the behavior of phononic systems.

In Fig. 3 we study energy transfer between metals employing a Lorentzian density of states of width γ, $D_\nu(\epsilon)=(\gamma/2\pi)/(\epsilon^2+\gamma/4^2)$. We observe a small negative differential thermal conductance, i.e., a decrease in the current with

increasing temperature difference at large temperature bias. The effect prevails when $\gamma \lesssim \omega$, i.e., the reservoir density of states is notably changing over the subsystem energy scale. The data were generated by employing Eq. (11) with the rate (23). The inset presents the F function (24), evaluated with the Lorentzian DOS.

Summarizing, while in pure harmonic systems nonlinear dynamics is linked to quantum effects (29), spin systems manifest nonlinear dynamics irrespective of the subsystem frequency [Eqs. (30) and (36)]. In a simple model for anharmonic vibrational heat flow (31), nonlinearities are attributed to the spatial asymmetry, while nonlinear effects in excitonic energy transfer are linked to the metals' energy dependent density of states (37). The conductance temperature dependence also varies. For harmonic systems it is independent of temperature, while for anharmonic phononic systems it decays like $1/T$, in general agreement with experimental results [56]. In metal–single-mode–metal junctions the conductance *increases* with temperature due to the enhancement of the transition rate with T.

With respect to NDTC, we note that it is not trivial to acquire the effect in weakly coupled junctions. Besides the metallic case (Fig. 3), the presented examples either yield positive expansion coefficients $\alpha_n > 0$ [see Eq. (28)] or an alternating-sign series, where the overall current grows with ΔT (33). In order to attain significant NDTC the rate constants, e.g., $k^L(T_a+\Delta T)$, should strongly *decrease* with increasing ΔT. This can be realized by using reservoirs with nonuniform density of states, as we showed above, or by going beyond the weak-coupling approximation [38].

F. Effective temperature

We would like next to suggest that a measurement of the subsystem temperature in a nonequilibrium situation could indicate the importance of nonlinear interactions in the transport process. Consider, for example, a single-mode junction, where the central object is modeled by a harmonic oscillator of frequency ω. Irrespective of the type of reservoirs and the form of interaction, we define next the central object *effective* temperature T_M through the relative levels occupation in steady state,

$$\frac{P_n}{P_{n-1}} = e^{-\omega/T_M}. \tag{38}$$

Since the system is out of equilibrium and, furthermore, the subsystem is a small-quantized object, T_M is not a temperature in the standard thermodynamic sense, yet it can be measured: in a recent experiment [57] a surface-enhanced Raman spectroscopy method was used to determine the nonequilibrium occupancy of vibrational modes and the effective (mode specific) temperature of current-carrying junctions. For harmonic subsystems for any pair of levels, we find that [38]

$$T_M = -\omega/\ln x, \tag{39}$$

where

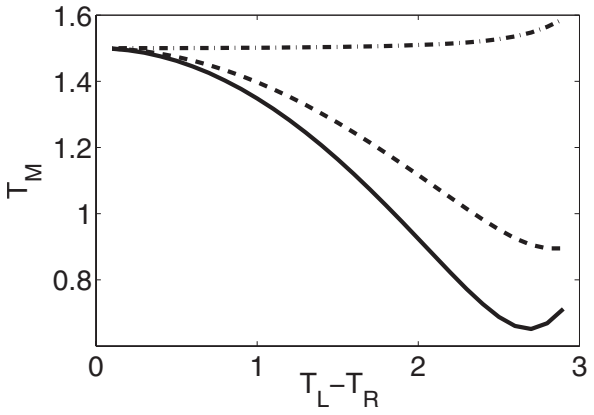

FIG. 4. Effective subsystem temperature in a metal–single-mode–metal junction with $\gamma=0.2$ (solid line), $\gamma=5$ (dashed line), and for linear metals, $\gamma \to \infty$ (dashed-dotted line). $\Gamma_F^L=\Gamma_F^R=1$, $T_a=3$, $\omega=0.5$.

$$x = \frac{k^L(T_L)e^{-\omega/T_L} + k^R(T_R)e^{-\omega/T_R}}{k^L(T_L) + k^R(T_R)}, \tag{40}$$

with the rate constants defined in Eq. (13). Assuming harmonic reservoirs and bilinear coordinate-coordinate interactions, e.g., the reservoirs are harmonic solids or linear electromagnetic media [11], we obtain the subsystem temperature

$$T_M = \frac{\omega}{\ln\left(1 + \dfrac{\Gamma_B^L + \Gamma_B^R}{\Gamma_B^L n_B^L + \Gamma_B^R n_B^R}\right)}. \tag{41}$$

In the classical limit this reduces to the algebraic average $T_M=(\Gamma_B^L T_L+\Gamma_B^R T_R)/(\Gamma_B^L+\Gamma_B^R)$. While in an equilibrium situation ($T_L=T_R$) T_M always approaches the reservoirs' temperature irrespective of the internal dynamics, in nonequilibrium situations a deviation from Eq. (41) might occur, indicating on the importance of nonlinear interactions in the transport process.

As an example, consider a metal–single-mode–metal junction as in Fig. 3. For the same data, we present in Fig. 4 the temperature T_M as defined in Eq. (38), using the rate constants (23) with a Lorentzian density of states of width γ, $D_\nu(\epsilon)=(\gamma/2\pi)/(\epsilon^2+\gamma/4^2)$. At large γ the reservoirs density of states is effectively constant, the reservoirs are linear, and the harmonic behavior is recovered (dashed-dotted line). In this case the departure of T_M from the classical $T_a/2$ value is due to the importance of quantum effects at low T_R. On the other hand, if the density of states strongly varies with energy (full line), reflecting deviations from the harmonic picture [39], a significant diversion from the harmonic behavior comes forth, and a substantial decrease in temperature (to half the harmonic value) is observed. It is interesting to note that while the heat current in Fig. 3 is linear in ΔT for a wide range of temperature differences, T_M is a more sensitive measure for the onset of nonlinear interactions.

V. THERMAL RECTIFICATION: SUFFICIENT CONDITIONS

We focus next on a specific nonlinear effect, thermal rectification, asymmetry of the heat current for forward, and reversed temperature difference, $|J(+\Delta T)| \neq |J(-\Delta T)|$. Formally, the onset of this phenomenon is identified by the existence of even terms, $\alpha_{k=2n} \neq 0$ $(n=1,2,\ldots)$, in expansion (28).

We discuss here sufficient conditions for thermal rectification by analyzing the currents in Eqs. (11) and (12). These expressions are naturally not the most general results for heat transfer across hybrid structures. Rather, they relay on few assumptions as explained in Sec. III: the subsystem and reservoirs are weakly interacting, the baths are assumed to be held at thermal equilibrium, and the dynamics is Markovian. Furthermore, specific forms for the subsystem are employed. However, these analytical forms, derived from a prototype model, can still illuminate on the basic mechanisms involved in thermal rectification. Having said so, we return to Eqs. (11) and (12) and analyze their structure for forward ($T_L=T_H$, $T_R=T_C$) and reversed ($T_L=T_C$, $T_R=T_H$) temperature gradients, $T_H>T_C$. We note that in each expression separately these currents deviate in magnitude if the denominators fulfill

$$\frac{n^H(-\omega)}{k^L(T_H)}+\frac{n^C(-\omega)}{k^R(T_C)} \neq \frac{n^C(-\omega)}{k^L(T_C)}+\frac{n^H(-\omega)}{k^R(T_H)}, \tag{42}$$

where n^ν is either the spin occupation factor or the Bose-Einstein distribution. Rearranging this expression and making use of Eq. (10), we get

$$\frac{n^H(-\omega)}{\lambda_L^2 f_L(T_H)}-\frac{n^H(-\omega)}{\lambda_R^2 f_R(T_H)} \neq \frac{n^C(-\omega)}{\lambda_L^2 f_L(T_C)}-\frac{n^C(-\omega)}{\lambda_R^2 f_R(T_C)}. \tag{43}$$

In what follows we identify two classes of rectifiers. In type-*A* rectifiers system-bath interactions are equivalent at both contacts, but the reservoirs have distinct properties. In type-*B* rectifiers the reservoirs are equivalent, but the subsystem statistics is distinct from the baths, combined with some parametric asymmetry.

A. Type-*A* thermal rectifier

The rate constants (13) can be expressed in terms of the reservoirs density of states. For example, the rate induced by the L contact is given by

$$k^L(T)=2\pi\lambda_L^2\sum_{l,l'}|B^L_{l,l'}|^2\delta(E_l-E_{l'}+\omega)\frac{e^{-\beta E_l}}{Z_L(\beta)}$$

$$=2\pi\lambda_L^2\frac{\int d\epsilon\, e^{-\beta\epsilon}D_L(\epsilon)g_L(\epsilon,\omega)}{\int d\epsilon\, e^{-\beta\epsilon}D_L(\epsilon)}. \tag{44}$$

Here, $Z_L(\beta)=\Sigma_l e^{-\beta E_l}=\int d\epsilon\, e^{-\beta\epsilon}D_L(\epsilon)$ denotes the partition function of the L bath with the density of states $D_L(\epsilon)=\Sigma_l\delta(\epsilon-E_l)$. The function $g_L(\epsilon,\omega)=\Sigma_l|B^L(\epsilon,E_l)|^2\delta(\epsilon-E_l+\omega)$ characterizes system-bath interactions. Taking $\lambda_L=\lambda_R$, we note that since the two sides of Eq. (43) depend on different temperatures, the system rectifies heat if

$$f_L(T) \neq f_R(T), \tag{45}$$

besides special points in the parameter space, depending on the details of the model. Using Eq. (44), this condition reduces to

$$\frac{\int d\epsilon\, e^{-\beta\epsilon}D_L(\epsilon)g_L(\epsilon,\omega)}{\int d\epsilon\, e^{-\beta\epsilon}D_L(\epsilon)} \neq \frac{\int d\epsilon\, e^{-\beta\epsilon}D_R(\epsilon)g_R(\epsilon,\omega)}{\int d\epsilon\, e^{-\beta\epsilon}D_R(\epsilon)}. \tag{46}$$

We next further assume that $g_L(\epsilon,\omega)=g_R(\epsilon,\omega)$, i.e., system-bath interaction matrix elements are equal at both ends. Hence, inequality (45) is satisfied when

$$D_L(\epsilon) \neq D_R(\epsilon). \tag{47}$$

We thus recover a sufficient condition for thermal rectification: the density of states of the reservoirs should be distinct. Note that at least one of the reservoirs should have an *energy-dependent* DOS. If both reservoirs are harmonic, $D_\nu=c_\nu$, with c_ν being a constant, rectification is absent even for $c_L \neq c_R$. It is thus sufficient to have one of the reservoirs incorporating anharmonic interactions. If both reservoirs are nonlinear, rectification takes place if the energy spectra are distinct. This discussion relays on the assumption that the spectral function $g(\epsilon,\omega)$ explicitly depends on energy; see Eq. (46) and [58].

Going back to condition (46), we Taylor expand the interaction function around ω, $g_\nu(\epsilon,\omega)\sim\alpha_1(\omega)+\alpha_2(\omega)\epsilon$,

$$\frac{\int d\epsilon\, e^{-\beta\epsilon}D_L(\epsilon)\epsilon}{\int d\epsilon\, e^{-\beta\epsilon}D_L(\epsilon)} \neq \frac{\int d\epsilon\, e^{-\beta\epsilon}D_R(\epsilon)\epsilon}{\int d\epsilon\, e^{-\beta\epsilon}D_R(\epsilon)}. \tag{48}$$

We identify the left- (right-) hand side as the average energy of the L (R) reservoir. This relation manifests that rectification exists if $\langle H_L^0\rangle \neq \langle H_R^0\rangle$ as in [40]. Specifically, consider interfaces including one-dimensional oscillator chains, $H_\nu^0=H_\nu^{kin}+H_\nu^{pot}$, where the kinetic energy H_ν^{kin} is quadratic in momentum, and the potential energy per particle is $C_n q^n$, where $n\geq 2$ and q is the particle's coordinate. In the classical limit using the equipartition relation, we obtain $\langle H_\nu^0\rangle=T_\nu(\frac{1}{2}+\frac{1}{n})$. Thermal rectification thus emerges if the reservoirs have a nonidentical power n. Note that the separation to three segments (L, subsystem, and R) is often artificial: the junction could be practically made of a single structure with a varying potential energy, e.g., a nanotube whose composition gradually changes in space [51], leading to inhomogeneous energy spectra, and thus to thermal rectification.

To conclude, rectification has been obtained here relying on the DOS asymmetry $D_L(\epsilon) \neq D_R(\epsilon)$, while system-bath interactions are assumed symmetric, $\lambda_L=\lambda_R$ and $g_L(\omega,\epsilon)=g_R(\omega,\epsilon)$, energy-dependent functions. This conclusion is in

accord with multitude (numerical) observations, demonstrating rectification in two-segment dissimilar anharmonic lattices [42–46].

B. Type-*B* thermal rectifier

We explore next the role of the subsystem statistics in inducing thermal rectification by further studying inequality (43). As discussed above, type-*A* rectifiers are constructed assuming that $f_L(T) \neq f_R(T)$, resulting from the use of dissimilar reservoirs. However, a more careful analysis of Eq. (43) reveals that rectification prevails even when $f(T) \equiv f_L(T) = f_R(T)$, as long as $\lambda_L \neq \lambda_R$ *and* the ratio $n^{\nu}(-\omega)/f_{L,R}(T_{\nu})$ depends on the temperature T_{ν}. We show it by rearranging Eq. (43),

$$\frac{n^H(-\omega)}{f(T_H)}\left(\frac{1}{\lambda_L^2}-\frac{1}{\lambda_R^2}\right) \neq \frac{n^C(-\omega)}{f(T_C)}\left(\frac{1}{\lambda_L^2}-\frac{1}{\lambda_R^2}\right). \tag{49}$$

In order for the two sides to deviate, the ratio, e.g., $n^H(-\omega)/f(T_H)$ must depend on the respective temperature. In other words, *the relaxation rates' temperature dependence should differ from the central unit particle statistics*. As shown in Sec. III B, the function $f_{\nu}(T)$ reflects the reservoirs statistics [see Eqs. (10) and (27)]. We therefore classify type-*B* rectifiers as junctions where subsystem and bath differ in their statistics, and the identical reservoirs are asymmetrically coupled to the subsystem $\lambda_L \neq \lambda_R$. This observation is in agreement with other studies. For example, in Ref. [39] rectification was demonstrated in a quantum-mechanical model where photon-mediated heat current flows between two (asymmetrically coupled) nonlinear reservoirs. Refs. [37,50] consider a nonlinear subsystem mode while the reservoirs are taken harmonic, yielding rectification due to the inclusion of some spatial asymmetry.

Summarizing, in type-*B* rectifiers the reservoirs and system-bath couplings are equal at both ends, $D_L(\epsilon)=D_R(\epsilon)$ and $g_L(\epsilon,\omega)=g_R(\epsilon,\omega)$, but (i) one of the contacts is weaker, $\lambda_L \neq \lambda_R$, and (ii) the subsystem statistics differs from the reservoirs' statistics.

C. Examples

In what follows we exemplify type-*A* and type-*B* rectifiers. The magnitude of thermal rectification can be estimated by the sum $\Delta J \equiv J_{\Delta T}+J_{-\Delta T}$, where $J_{\pm\Delta T}=J(T_L-T_R=\pm\Delta T)$, or by the ratio $\mathcal{R} \equiv |J_{\Delta T}/J_{-\Delta T}|$. As expected from our general analysis above, a fully harmonic system (29), a pure spin system (30), and a uniform 3LS model (36) do not rectify heat *irrespective of the spatial asymmetry* embodied in $\chi \neq 0$, since (i) the DOS of both contacts are equal and (ii) subsystem and baths are equivalent. This should be emphasized since the latter two cases can be viewed as anharmonic structures due to the truncated energy spectra. In contrast, for a harmonic bath-TLS-harmonic bath junction (31), we obtain the ratio

$$\mathcal{R} \sim 1 - 2\frac{\Delta T}{T_a}\chi_B. \tag{50}$$

Similarly, for a metal–single-mode–metal junction, using Eq. (37) at small δ, we find

$$\mathcal{R} \sim 1 - \frac{\delta}{\mu}\chi_F \Delta T. \tag{51}$$

Thus, in type-*B* rectifiers the strength of the effect is directly linked to the spatial asymmetry, $\chi \neq 0$ [37,39].

We demonstrate next some type-*A* rectifiers, where the reservoirs have distinct properties. In order to simplify the presentation we set $\Gamma=\Gamma_B^L=\Gamma_S^R$, i.e., the central unit is evenly coupled to the reservoirs. Our first example is a phonon bath-HO-spin bath junction, representing e.g., an insulating molecule interfacing a dielectric surface and a nuclear-spin environment. For a schematic representation see Fig. 1(a). The current is calculated using Eq. (11) with rates (16) and (19) resulting in

$$J = \Gamma\omega\frac{n_B^L(\omega)-n_B^R(\omega)}{1-\dfrac{n_B^R(-\omega)}{n_S^R(-\omega)}}. \tag{52}$$

The magnitude of thermal rectification is

$$\mathcal{R} = \frac{n_B^H(-\omega)}{n_B^C(-\omega)} = \frac{1-\exp\left(-\dfrac{2\omega}{T_a-\Delta T}\right)}{1-\exp\left(-\dfrac{2\omega}{T_a+\Delta T}\right)}. \tag{53}$$

It is easy to see that, when $2\omega/(T_a \pm \Delta T) \gg 1$, the rectifier is effectively turned off while for $2\omega/(T_a \pm \Delta T) \ll 1$ it is operative, with $\mathcal{R} \sim 1+2\Delta T/T_a$.

Our second example is a phonon bath-HO-metal junction, representing an electronic to vibrational energy conversion device [see Fig. 1(b)]. This system can be realized in a metal-molecule contact, where the vibrational decay into the lead (e.g., an STM tip) is bottlenecked by a single vibrational mode. Setting the coupling strength at both contacts to be the same, $\Gamma=\Gamma_B^L=\Gamma_F^R$, we get

$$J = \omega\Gamma\frac{n_B^L(\omega)-n_B^R(\omega)}{1+\left(1+\delta_R\dfrac{T_R}{\mu_R}\right)^{-1}}, \tag{54}$$

with the rectification ratio

$$\mathcal{R} = \frac{\left(2+\delta_R\dfrac{T_H}{\mu_R}\right)\left(1+\delta_R\dfrac{T_C}{\mu_R}\right)}{\left(1+\delta_R\dfrac{T_H}{\mu_R}\right)\left(2+\delta_R\dfrac{T_C}{\mu_R}\right)} \sim 1-\delta_R\frac{\Delta T}{2\mu_R}. \tag{55}$$

This expression is similar to Eq. (51). However, since here the reservoirs are distinct (effectively $\delta_L=0$, $\delta_R \neq 0$), rectification is obtained for $\chi=0$.

Figure 5 presents a similar instance, vibrations to electronic excitations energy exchange, mediated by the excitation of an *anharmonic molecular* (TLS) mode. Interestingly, for small ω the solid transfers heat to the metal more effectively that the reversed metal-to-dielectric process, reflected by a rectification ratio larger than 1. For large spacing the behavior is reversed, and the metal better cools down. Consequently, there is an intermediate value ($\omega \sim 3$ for $\delta_F^R=0.4$) where this nonlinear-inhomogeneous junction does not rec-

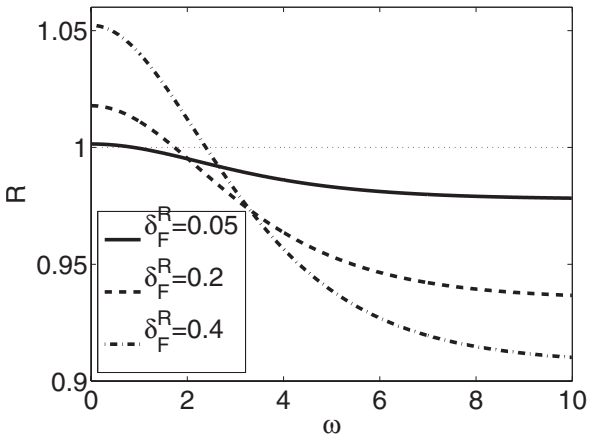

FIG. 5. Electronic to vibrational energy exchange through a TLS mode with δ_R=0.05 (solid line), δ_R=0.2 (dashed line), and δ_R=0.4 (dashed-dotted line). Rectification ratio is presented as a function of the subsystem energy spacing. T_a=3, ΔT=1, μ_R=1, Γ_B^L=Γ_F^R=1.

tify heat. The rectification ratio obtained here is relatively small, since the metal only weakly deviates from the Ohmic description [39]. This example still demonstrates that by optimizing system and interface parameters it may be possible to design a junction where the electron bath can be rapidly cooled down, while the vibrational energy ineffectively dissipates into the metallic bulk, and vice versa.

Finally, we examine a spin-subsystem-metal junction. In Fig. 6 we show that it can rectify heat in the classical limit ($\omega < T_\nu$) while in the quantum regime rectification is suppressed. We also modify the system-metal coupling strength and show that it can largely control the rectification ratio (inset).

VI. SUMMARY

This paper provided a unified description of heat flow in two-terminal hybrid structures assuming weak system-bath couplings. The underlying origin of nonlinear behavior in various junctions, and its controllability, were explored considering different interfaces—metals, insulators, and noninteracting spins—where the central object (subsystem) could represent, e.g., a radiation mode or a vibrational excitation.

As a particular example of nonlinear conduction we examined thermal rectification. Previous studies of this effect were typically based on numerics, utilizing classical molecular-dynamics tools, where observations were deduced within specific molecular force fields [41–48]. Here, in contrast, we attempted a general analytical study of the sufficient conditions for the onset of thermal rectification in hybrid quantum models. We identified two classes of rectifiers: type-*A* rectifiers, where the interfaces are made distinct, and type-*B* rectifiers, where the reservoirs are equivalent, but the system and bath quantum statistics differ, in conjunction with some spatial (parametric) asymmetry. We note that the importance of anharmonicity and asymmetry for manifesting rectification were previously recognized, e.g., in a spin-boson model [37], yet the necessity of the inhomogeneity of the energy spectra was not appreciated. Here, we clearly observe that a system composed of identical *anharmonic* units cannot rectify heat, unless the energy spectra are made *nonuniform*, in conjunction with some spatial asymmetry.

Our study aims to link transport characteristics to the microscopic Hamiltonian. It might serve as a guide for experimentalists pursuing control over energy transfer in molecular systems [4,7,8,55] and for building nanoscale thermal devices [59,60]. We have also demonstrated that nonlinear thermal effects, and in particular thermal rectification, are ubiquitous phenomena that could be observed in a variety of systems—phononic [51], electronic [52], and photonic [11,39,54].

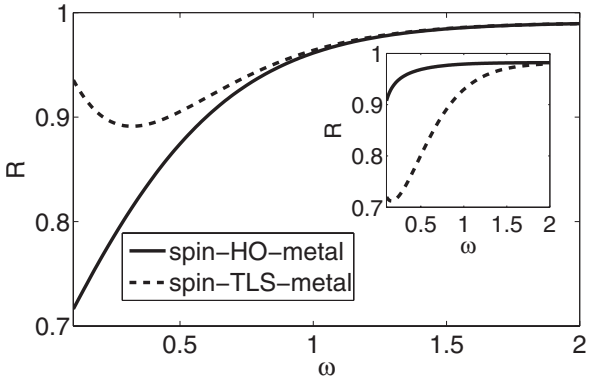

FIG. 6. Spin-HO-metal rectifier (solid line) and a spin-TLS-metal rectifier (dashed line). The rectification ratio is presented as a function of the subsystem energy spacing. T_a=0.5, ΔT=0.1, δ_R=0.2, μ_R=1. Main plot: the subsystem is equally coupled to the two ends, Γ_S^L=Γ_F^R=1. Inset: $\mathcal{R}$ can be tuned by manipulating system-bath interactions; Γ_S^L=1, Γ_F^R=0.05.

ACKNOWLEDGMENTS

This work was supported by NSERC and by the University of Toronto Start-up Funds. L.-A.W. acknowledges support from the Ikerbasque Foundation.

APPENDIX: DERIVATION OF THE HEAT CURRENT EXPRESSION WITHIN THE MASTER-EQUATION FORMALISM

The aim of this appendix is to derive the heat current expression (8) within the Hamiltonian (4). The expectation value of the current is formally given by

$$J = \mathrm{Tr}[\hat{J}\rho], \quad \hat{J} = \frac{i}{2}[V_L, H_S] + \frac{i}{2}[H_S, V_R]. \tag{A1}$$

Using the Hamiltonian (4) we get

$$J = \frac{i}{2}\sum_{n,m} E_{n,m} S_{m,n}\, \mathrm{Tr}_B[\lambda_L \rho_{n,m} B_L]$$

$$- \frac{i}{2}\sum_{n,m} E_{n,m} S_{m,n}\, \mathrm{Tr}_B[\lambda_R \rho_{n,m} B_R], \tag{A2}$$

where $E_{n,m}$=E_n−E_m, Tr_B denotes trace over the L and the R

baths, and ρ is the total density matrix whose elements should be calculated in the long-time limit since expression (A1) is valid in steady-state situations only [53]. We find it useful to rearrange Eq. (A2) as follows:

$$J = \frac{i}{2}\sum_{n>m} E_{n,m}S_{m,n}\,\mathrm{Tr}_B[\lambda_L(\rho_{n,m}-\rho_{m,n})B_L] - \frac{i}{2}\sum_{n>m} E_{n,m}S_{m,n}\,\mathrm{Tr}_B[\lambda_R(\rho_{n,m}-\rho_{m,n})B_R]. \quad \text{(A3)}$$

We would like to express the current in terms of the long-time population P_n. The Liouville equation of motion for $\rho_{n,m}$ is

$$\dot{\rho}_{n,m} = -iE_{n,m}\rho_{n,m} - i\sum_{\nu}\sum_{p}\lambda_\nu[B_\nu(t)S_{n,p}\rho_{p,m}(t) - S_{p,m}\rho_{n,p}(t)B_\nu(t)], \quad \text{(A4)}$$

with the transformed operators $B_\nu(t)=e^{iH_\nu t}B_\nu e^{-iH_\nu t}$ $(\nu=L,R)$. The index p counts the subsystem states. This equation can be formally integrated to yield

$$\rho_{n,m}(t) = -i\int_0^t e^{-iE_{n,m}(t-\tau)}\left[\sum_{\nu,p}\lambda_\nu B_\nu(\tau)S_{n,p}\rho_{p,m}(\tau) - \sum_{\nu,p}\lambda_\nu S_{p,m}\rho_{n,p}(\tau)B_\nu(\tau)\right]d\tau. \quad \text{(A5)}$$

The initial condition was already neglected since it will not contribute after tracing out the bath in Eq. (A3), assuming $\mathrm{Tr}_B[B(t),\rho(0)]=0$, i.e., the mean value of the interaction Hamiltonian, averaged over the initial density matrix, is zero. Plugging Eq. (A5) into Eq. (A3), we obtain λ^2 order terms. Factorizing the density matrix at all times, $\rho(t)=\rho_L(T_L)\rho_R(T_R)\sigma(t)$, $\rho_\nu(T_\nu)=e^{-H_\nu^0/T_\nu}/\mathrm{Tr}_\nu[e^{-H_\nu^0/T_\nu}]$, where $\sigma(t)=\mathrm{Tr}_B[\rho(t)]$, and taking the Markovian limit, replacing $\sigma(\tau)\to\sigma(t)$, we get

$$\mathrm{Tr}_B[\rho_{n,m}(t)B_L(t)] \approx -i\lambda_L\sum_p\int_0^t e^{-iE_{n,m}(t-\tau)}\times[\langle B_L(t)B_L(\tau)\rangle_{T_L}\sigma_{p,m}(t)S_{n,p} - \langle B_L(\tau)B_L(t)\rangle_{T_L}\sigma_{n,p}(t)S_{p,m}]d\tau. \quad \text{(A6)}$$

Here, $\langle B_\nu(\tau)B_\nu(0)\rangle_{T_\nu}\equiv\mathrm{Tr}_\nu[\rho_\nu(T_\nu)B_\nu(\tau)B_\nu(0)]$ is the correlation function of the ν environment. In deriving Eq. (A6) we disregarded mixed terms of the form $\langle B_L(t)B_R(\tau)\rangle$, since the terminals are not correlated. Our next assumption is that coherences are negligible in the weak-coupling scheme, given the preparation $\sigma_{n\neq m}(0)\sim 0$; thus, we disregard all the nondiagonal terms in Eq. (A6). Further, performing the transformation $x=\tau-t$ and extending the integral to infinity (Markovian approximation), we obtain

$$\mathrm{Tr}_B[\rho_{n,m}(t)B_L(t)] \approx -i\lambda_L\int_0^\infty e^{iE_{n,m}x}\times[\langle B_L(0)B_L(x)\rangle_{T_L}\sigma_{m,m}(t)S_{n,m} - \langle B_L(x)B_L(0)\rangle_{T_L}\sigma_{n,n}(t)S_{n,m}]dx. \quad \text{(A7)}$$

Similarly, we find that

$$\mathrm{Tr}_B[\rho_{m,n}(t)B_L(t)] \approx -i\lambda_L\int_{-\infty}^0 e^{iE_{n,m}x}\times[\langle B_L(x)B_L(0)\rangle_{T_L}\sigma_{n,n}(t)S_{m,n} - \langle B_L(0)B_L(x)\rangle_{T_L}\sigma_{m,m}(t)S_{m,n}]dx. \quad \text{(A8)}$$

Combining the last two expressions, we come by (using $S_{n,m}=S_{m,n}$)

$$\mathrm{Tr}_B\{[\rho_{n,m}(t)-\rho_{m,n}(t)]B_L(t)\} \approx i\lambda_L S_{n,m}\left[P_n(t)\int_{-\infty}^\infty e^{iE_{n,m}x}\langle B_L(x)B_L(0)\rangle_{T_L} - P_m(t)\int_{-\infty}^\infty e^{iE_{n,m}x}\langle B_L(0)B_L(x)\rangle_{T_L}\right]. \quad \text{(A9)}$$

We return now to the heat current expression (A3) and identify the ν-bath-induced relaxation rates by

$$k^\nu_{n\to m}(T_\nu) = \lambda_\nu^2\int_{-\infty}^\infty d\tau\, e^{iE_{n,m}\tau}\langle B_\nu(\tau)B_\nu(0)\rangle_{T_\nu}. \quad \text{(A10)}$$

By making use of Eq. (A9), conjoined with the analogous R-bath expression, we get a weak-coupling expression for the heat current, defined positive when flowing from L to R,

$$J = -\frac{1}{2}\sum_{n>m}E_{n,m}|S_{m,n}|^2[P_n k^L_{n\to m}(T_L) - P_m k^L_{m\to n}(T_L)] + \frac{1}{2}\sum_{n>m}E_{n,m}|S_{m,n}|^2[P_n k^R_{n\to m}(T_R) - P_m k^R_{m\to n}(T_R)], \quad \text{(A11)}$$

or more compactly

$$J = \frac{1}{2}\sum_{n,m}E_{m,n}|S_{n,m}|^2P_n[k^L_{n\to m}(T_L) - k^R_{n\to m}(T_R)]. \quad \text{(A12)}$$

This is our final result, a second-order (λ^2) expression for the heat current, obtained within the master-equation approach. The populations P_n should be calculated at long time using Eq. (6).

[1] D. G. Cahill *et al.*, J. Appl. Phys. **93**, 793 (2003).
[2] V. P. Carey *et al.*, Nanoscale Microscale Thermophys. Eng. **12**, 1 (2008).
[3] D. Segal and A. Nitzan, J. Chem. Phys. **117**, 3915 (2002); Y. C. Chen, M. Zwolak, and M. Di Ventra, Nano Lett. **3**, 1691 (2003); M. Galperin, A. Nitzan, and M. A. Ratner, Phys. Rev. B **75**, 155312 (2007).
[4] G. Schulze *et al.*, Phys. Rev. Lett. **100**, 136801 (2008).
[5] Z. Huang *et al.*, Nat. Nanotechnol. **2**, 698 (2007).
[6] H. Fujisaki and J. E. Straub, Proc. Natl. Acad. Sci. U.S.A. **102**, 6726 (2005).
[7] V. Botan *et al.*, Proc. Natl. Acad. Sci. U.S.A. **104**, 12749 (2007).
[8] Z. Wang *et al.*, Science **317**, 787 (2007).
[9] F. Bonetto, J. Lebowitz, and L. Rey-Bellet, *Mathematical Physics 2000* (World Scientific, Singapore, 2000), p. 128150.
[10] C. W. Chang, D. Okawa, H. Garcia, A. Majumdar, and A. Zettl, Phys. Rev. Lett. **101**, 075903 (2008).
[11] M. Meschke, W. Guichard, and J. P. Pekola, Nature (London) **444**, 187 (2006).
[12] J. M. Taylor, C. M. Marcus, and M. D. Lukin, Phys. Rev. Lett. **90**, 206803 (2003).
[13] B. N. J. Persson and H. Ueba, Phys. Rev. B **76**, 125401 (2007).
[14] F. Giazotto *et al.*, Rev. Mod. Phys. **78**, 217 (2006).
[15] S. Lepri, R. Livi, and A. Politi, Phys. Rep. **377**, 1 (2003).
[16] A. Dhar, Adv. Phys. **57**, 457 (2008).
[17] C. Mejia-Monasterio, T. Prosen, and G. Casati, EPL **72**, 520 (2005).
[18] M. Michel, G. Mahler, and J. Gemmer, Phys. Rev. Lett. **95**, 180602 (2005).
[19] M. Michel, J. Gemmer, and G. Mahler, Int. J. Mod. Phys. B **20**, 4855 (2006).
[20] L.-A. Wu and D. Segal, Phys. Rev. E **77**, 060101(R) (2008).
[21] J.-S. Wang, J. Wang, and J. T. Lü, Eur. Phys. J. B **62**, 381 (2008).
[22] G. Benenti, G. Casati, T. Prosen, and D. Rossini, EPL **85**, 37001 (2009).
[23] L. G. C. Rego and G. Kirczenow, Phys. Rev. Lett. **81**, 232 (1998).
[24] D. Segal, A. Nitzan, and P. Hänggi, J. Chem. Phys. **119**, 6840 (2003).
[25] A. Dhar and D. Roy, J. Stat. Phys. **125**, 801 (2006).
[26] H. Spohn, J. Stat. Phys. **124**, 1041 (2006).
[27] L. Delfini, S. Lepri, R. Livi, and A. Politi, Phys. Rev. E **73**, 060201(R) (2006); J. Stat. Mech.: Theory Exp. **2007**, P02007 (2007).
[28] J.-S. Wang and B. Li, Phys. Rev. E **70**, 021204 (2004).
[29] N. Mingo and L. Yang, Phys. Rev. B **68**, 245406 (2003); N. Mingo, *ibid.* **74**, 125402 (2006).
[30] J.-S. Wang, J. Wang, and N. Zeng, Phys. Rev. B **74**, 033408 (2006); J.-S. Wang, N. Zeng, J. Wang, and C. K. Gan, Phys. Rev. E **75**, 061128 (2007).
[31] J.-S. Wang, Phys. Rev. Lett. **99**, 160601 (2007).
[32] K. A. Velizhanin, H. Wang, and M. Thoss, Chem. Phys. Lett. **460**, 325 (2008).
[33] H.-P. Breuer and F. Petruccione, *The Theory of Open Quantum Systems* (Oxford University Press, New York, NY, 2002).
[34] H. Wichterich, M. J. Henrich, H. P. Breuer, J. Gemmer, and M. Michel, Phys. Rev. E **76**, 031115 (2007).
[35] Y. Yan, C. Q. Wu, G. Casati, T. Prosen, and B. Li, Phys. Rev. B **77**, 172411 (2008).
[36] Y. Dubi and M. Di Ventra, Phys. Rev. B **79**, 115415 (2009).
[37] D. Segal and A. Nitzan, Phys. Rev. Lett. **94**, 034301 (2005); J. Chem. Phys. **122**, 194704 (2005).
[38] D. Segal, Phys. Rev. B **73**, 205415 (2006).
[39] D. Segal, Phys. Rev. Lett. **100**, 105901 (2008).
[40] L.-A. Wu and D. Segal, Phys. Rev. Lett. **102**, 095503 (2009).
[41] M. Terraneo, M. Peyrard, and G. Casati, Phys. Rev. Lett. **88**, 094302 (2002).
[42] B. Li, L. Wang, and G. Casati, Phys. Rev. Lett. **93**, 184301 (2004); B. Li, J. H. Lan, and L. Wang, *ibid.* **95**, 104302 (2005).
[43] B. Hu, L. Yang, and Y. Zhang, Phys. Rev. Lett. **97**, 124302 (2006).
[44] J. Lan and B. Li, Phys. Rev. B **74**, 214305 (2006).
[45] J. H. Lan and B. Li, Phys. Rev. B **75**, 214302 (2007).
[46] N. Yang, N. Li, L. Wang, and B. Li, Phys. Rev. B **76**, 020301(R) (2007).
[47] N. Zeng and J.-S. Wang, Phys. Rev. B **78**, 024305 (2008).
[48] G. Casati, C. Mejia-Monasterio, and T. Prosen, Phys. Rev. Lett. **98**, 104302 (2007).
[49] E. Pereira and H. C. F. Lemos, Phys. Rev. E **78**, 031108 (2008).
[50] T. Ruokola, T. Ojanen, and A.-P. Jauho, Phys. Rev. B **79**, 144306 (2009).
[51] C. W. Chang, D. Okawa, A. Majumdar, and A. Zettl, Science **314**, 1121 (2006).
[52] R. Scheibner *et al.*, New J. Phys. **10**, 083016 (2008).
[53] L.-A. Wu and D. Segal, J. Phys. A: Math. Theor. **42**, 025302 (2009).
[54] T. Ojanen and A. P. Jauho, Phys. Rev. Lett. **100**, 155902 (2008).
[55] T. Kodama, A. Jain, and K. E. Goodson, Nano Lett. **9**, 2005 (2009).
[56] E. Pop *et al.*, Nano Lett. **6**, 96 (2006).
[57] Z. Ioffe *et al.*, Nat. Nanotechnol. **3**, 727 (2008).
[58] The function $g_\nu(\epsilon,\omega)$ typically depends on energy. For example, for $B\propto(a^\dagger+a)$ as in Eq. (18), $|B_{ll'}|^2\propto l\delta_{l',l-1}+(l+1)\delta_{l',l+1}$
[59] B. Li, L. Wang, and G. Casati, Appl. Phys. Lett. **88**, 143501 (2006); L. Wang and B. Li, Phys. Rev. Lett. **99**, 177208 (2007); **101**, 267203 (2008).
[60] C. W. Chang *et al.*, Appl. Phys. Lett. **90**, 193114 (2007).